

## ANALYTICAL CROSS SECTIONS AND RATE COEFFICIENTS FOR H-H INELASTIC COLLISIONS

W. H. SOON

Harvard-Smithsonian Center for Astrophysics, 60 Garden Street, Cambridge, MA 02138

*Received 1992 January 3; accepted 1992 February 6*

### ABSTRACT

Analytical expressions for cross sections and the corresponding Maxwellian rate coefficients for direct excitation and ionization in binary collisions of hydrogen atoms are evaluated by using the classical impulse approximation. The maximum values of the ionization and excitation cross sections and the positions of the maxima are also predicted. The classical impulse approximation cross sections were compared with available measurements and quantum-mechanical cross sections. The classical impulse approximation rate coefficients calculated were compared to the commonly used semi-empirical rate coefficients of Drawin. The comparison indicates that the commonly used semi-empirical rate coefficients are significantly higher than the classical impulse approximation rates for excitation and ionization transitions from excited levels.

*Subject headings:* atomic data — atomic processes

### 1. INTRODUCTION

Almost all previous works on H-H excitation and ionization collisions give the corresponding cross sections in an energy range that is unsuitable for evaluation of the excitation and ionization rate coefficients at temperatures  $10^2 \text{ K} \leq T \leq 10^6 \text{ K}$  (see, for example, Omidvar & Kyle 1970 and Pomella 1967). Such cross sections and rate coefficients are of interest in the analysis of hydrogen emission lines from supernova remnants (SNRs) (see, for example, Smith et al. 1991). Modeling of low-temperature laboratory hydrogen plasmas also requires reliable cross sections and rate coefficients for H-H inelastic collisions (see, for example, Kunc 1987). Using the classical impulse approximation, we obtain here a consistent set of cross sections and rate coefficients for the direct H-H excitation and ionization collisions. By direct, we mean H-H collisions in which one atom remains in the ground state and the other is either excited or ionized. Double-transition collisions when the target atom is either excited or ionized with a simultaneous excitation or ionization of the incident atom have been discussed (see, for example, Bates & Griffing 1954, 1955; Pomella & Milford 1966, Levy 1969; Flannery 1972, 1973; McLaughlin & Bell 1983, 1989) and it was shown that their contribution to the total cross sections is unimportant, compared to the contribution of the direct collision for impact energies  $E \lesssim 10\text{--}20 \text{ keV}$ .

In our previous work (Kunc & Soon 1991, hereafter Paper I), general analytical cross sections for direct ionization in atom-atom collisions were derived within the frame of the classical impulse approximation. The purpose of this work is to focus on the application of the classical impulse approximation to inelastic collisions of two hydrogen atoms



and the calculations of the cross sections and rate coefficients.

In the next section, the derivation of the classical impulse approximation cross sections and rate coefficients is presented. Then several of the available rate coefficients (the parameters that are most directly relevant in application) in the literature are briefly discussed. The results presented in this work can be divided into two parts. First, the classical impulse approx-

imation cross sections are compared with available measurements and quantum mechanical calculations, to assess the reliability of the classical impulse approximation cross sections. Then the rate coefficients, calculated using the classical impulse approximation cross sections, are compared with other results.

### 2. CLASSICAL IMPULSE APPROXIMATION IONIZATION AND EXCITATION CROSS SECTIONS AND RATE COEFFICIENTS

The atom-atom interaction is taken here as a superposition of all the pairwise interactions between the so-called test particle (a structureless object representing the average dynamical properties of all the components of the incident atom) and the electron (the so-called field electron) of the target atom. Details on the derivation of the ionization cross sections are given in Paper I. We have also extended the work in Paper I to evaluate the corresponding classical impulse approximation cross sections for the direct excitation in H-H collisions. Although it seems to be conceptually more difficult to justify the application of the classical impulse approximation to the description of the excitation collisions, we nevertheless include the results from it in the present work because of its simplicity and its reasonable comparison with measurements (see below). The cross sections for the direct ionization for the  $n$ th energy level of the target atom to continuum (process 1) and for the direct excitation from a lower level  $n$  of the target atom to an upper level  $n'$  (process 2) is given by

$$Q_{nc}^{\text{H}}(E) = \pi \left( \frac{r_a}{r_b} \right)^2 \left( \frac{e^2}{[U_n + (m_e/m_{\text{H}})E]} \right)^2 \times \left[ \frac{1}{U_n} - \frac{1}{U_n + (4m_e/m_a)(E - U_n)} \right] \times \sqrt{1 + \frac{m_{\text{H}} U_n}{m_e E} \left( \frac{m_e}{m_{\text{H}}} \right) (E - U_n)}, \quad (3)$$

$$Q_{nn'}^{\text{H}}(E) = \pi \left( \frac{r_a}{r_b} \right)^2 \left( \frac{e^2}{[U_n + (m_e/m_{\text{H}})E]} \right)^2 \left( \frac{1}{\epsilon_l} - \frac{1}{\epsilon_u} \right) \times \sqrt{1 + \frac{m_{\text{H}} U_n}{m_e E} \left( \frac{m_e}{m_{\text{H}}} \right) (E - U_n)} \quad E > U_n, \quad (4)$$

where  $E$  is the impact energy,  $U_n$  is the ionization potential of the target atom excited to the  $n$ th level,  $e$  is the electron charge,  $a_0$  is the Bohr radius,  $m_e$ , and  $m_H$  are masses of electron and atomic hydrogen, respectively, the efficiency factor  $\Omega = (r_a/r_b)^2$  and the limits of the energy transfer  $\epsilon_i$  and  $\epsilon_u$  are discussed below.

Since the collision of two atoms is represented here by interactions of two mass points, the test particle and the field electron, our model does not account for the fact that the probability of these two points to “meet” at a given impact parameter  $D$  depends on the magnitude of the relative “sizes” of the colliding atoms (or, more precisely, on the values of the radii of the atomic outer shells). (One should notice that in general the impact parameter  $D$  for the test particle-field electron interaction can be different from the impact parameter  $d$  for the centers of the colliding atoms). In other words, it is less probable during an atom-atom collision at a given  $d$  for the test particle to “find” the field electron excited to a higher state than to a lower state because in the former case the field electron orbit is larger. Taking the efficiency factor  $\Omega$  (representing the relative efficiency of the test particle to “find” the field electron) as equal to one when the outer shell radii of the colliding atoms are identical, this factor is proportional to the ratio of the geometrical cross sections of the atoms,  $\pi r_a^2/\pi r_b^2 = (r_a/r_b)^2$ , where  $r_a$  and  $r_b$  are the mean radii of the outer shells of the incident and the target hydrogen atom, respectively, given by  $r_n = n^2 a_0$ .

For the  $n \rightarrow c$  ionization transition, the energy threshold is  $\epsilon_i = U_n$  and the upper limit to the energy transfer is  $\epsilon_u = \epsilon_i + \kappa E' = U_n + \kappa(E - U_n)$  (see Paper I), where  $\kappa = (4m_e m_H)/(m_e + m_H)^2 = 4m_e/m_H$ . For  $n \rightarrow n'$  excitation transition, the energy threshold is  $\epsilon_i = \Delta E_{nn'}$  and the upper limit to the energy transfer is

$$\epsilon_u = \begin{cases} \epsilon_i + \kappa(E - U_n) = \Delta E_{nn'} + \kappa(E - U_n) & \text{when } E \leq U_n + \Delta E_{n',n'+1}/\kappa \\ \epsilon_i + \Delta E_{n',n'+1} = \Delta E_{n,n'+1} & \text{when } E > U_n + \Delta E_{n',n'+1}/\kappa, \end{cases} \quad (5)$$

where  $\Delta E_{n,n'}$  is the gap for the transition from the  $n$  level to the  $n'$  level. In the case of excitation, the cross sections (4) lose their validity at impact energies  $\Delta E_{nn'} \leq E \lesssim U_n$  because in our collision model the relative energy ( $E - U_n$ ) of the interaction between the test particle and the field electron is negative in such a case (see Paper I).

From the analytical ionization and excitation cross sections given by Equations (3) and (4), one can derive the corresponding maxima of the cross sections. The maximum values of the cross sections are given by

$$Q_{nc}^{\max}(E_n^*) = \frac{4\sqrt{2}\pi a_0^2}{5}, \quad (6)$$

$$Q_{nn'}^{\max}(E_{nn'}^*) = \frac{8\pi a_0^2}{3^{3/2}} \left\{ \frac{n^2(2n' + 1)}{(n'^2 - n^2)[(n' + 1)^2 - n^2]} \right\}, \quad (7)$$

and the energies corresponding to the maxima are

$$E_{nc}^* = \frac{m_H}{m_e} U_n, \quad (8)$$

$$E_{nn'}^* = \frac{m_H}{2m_e} U_n. \quad (9)$$

The maxima of the cross sections  $Q_{nc}$  and  $Q_{nn'}$  occur when the incident projectile velocity is roughly equal to the field electron velocity. The maxima of the predicted H-H ionization cross sections are independent of  $n$  and have a constant value (see discussion below) while the maximum values of the excitation cross sections depend on the principal quantum numbers  $n$  and  $n'$  of the initial and final states of the transitions.

In the low-energy region [ $U_n < E \ll (m_H/m_e)U_n$ ], the explicit dependence of the ionization and excitation cross sections on the principal quantum numbers of the transitions is as follows:

$$Q_{nc}^H(E) \approx 16\pi a_0^2 \left( \frac{m_e}{m_H} \right)^{3/2} \sqrt{\frac{Ry}{E}} \left( \frac{E}{Ry} - \frac{1}{n^2} \right)^2 n^3, \quad (10)$$

$$Q_{nn'}^H(E) \approx 16\pi a_0^2 \left( \frac{m_e}{m_H} \right)^{3/2} \sqrt{\frac{Ry}{E}} \left( \frac{E}{Ry} - \frac{1}{n^2} \right)^2 \left[ \frac{n^3 n'^4}{(n'^2 - n^2)^2} \right], \quad (11)$$

where  $Ry$  is the Rydberg. In the high-energy region [ $E \gg (m_H/m_e)U_n$ ], the explicit dependence of ionization and excitation cross sections on the principal quantum number of the transitions is as follows:

$$Q_{nc}^H(E) \approx 4\pi a_0^2 \frac{m_H Ry}{m_e E} \frac{1}{n^2}, \quad (12)$$

$$Q_{nn'}^H(E) \approx 4\pi a_0^2 \frac{m_H Ry}{m_e E} \left\{ \frac{(2n' + 1)}{(n'^2 - n^2)[(n' + 1)^2 - n^2]} \right\}. \quad (13)$$

The ionization and excitation rate coefficients are calculated by integrating the cross section over the Maxwellian distribution:

$$R(T) = \frac{8\pi}{\mu^2} \left( \frac{\mu}{2\pi kT} \right)^{3/2} \int_{E_{\min}}^{\infty} Q(E) \exp\left(-\frac{E_{\text{cm}}}{kT}\right) E_{\text{cm}} dE_{\text{cm}}, \quad (14)$$

where  $E_{\text{cm}} (= E/2)$  is the relative kinetic energy in the center of mass frame,  $E_{\min}$  is the threshold energy,  $Q(E = 2E_{\text{cm}})$  is the corresponding cross section, and  $\mu = m_H/2$  is the reduced mass of the colliding system.

The rate coefficients can be calculated either by direct numerical integration or by the following analytical approximation. First, the low-energy part of the cross section is studied; it is proportional to  $E^{3/2}$  (see eqs. [10] and [11]). Then, the upper and lower bounds of the integral in the relationship (14) can be evaluated analytically. Consequently, approximate formulae for the direct ionization ( $n \rightarrow c$ ) and excitation ( $n \rightarrow n'$ ) rate coefficients can be given as

$$S_{nc}^H(T) = \frac{64a_0^2}{\pi m_H^2} \left( \frac{\pi m_H}{kT} \right)^{3/2} \left( \frac{Ry}{U_n} \right)^2 \times \left( \frac{r_a}{r_b} \right)^2 \left( \frac{m_e}{m_H} \right)^{3/2} \left( \frac{U_n}{kT} \right) \Phi(\epsilon_i, kT), \quad (15)$$

$$S_{nn'}^H(T) = \frac{64a_0^2}{\pi m_H^2} \left( \frac{\pi m_H}{kT} \right)^{3/2} \left( \frac{Ry}{U_n} \right)^2 \left( \frac{r_a}{r_b} \right)^2 \times \left( \frac{m_e}{m_H} \right)^{3/2} \left( \frac{U_n}{kT} \right) \left( \frac{\Delta E_{nn'}}{kT} \right)^{1/2} \Phi(\epsilon_i, kT), \quad (16)$$

where

$$\Phi(\epsilon_i, kT) = \Phi_1 + \Phi_2 - \Phi_3, \quad (17)$$

$$\Phi_1 = \frac{4}{\epsilon_i^2} \exp\left(-\frac{U_n}{2kT}\right) F(j_1 = 3), \quad (18)$$

$$\Phi_2 = \frac{U_n^2}{\epsilon_i^2} \exp\left(-\frac{U_n}{2kT}\right) F(j_2 = 1), \quad (19)$$

$$\Phi_3 = \frac{4U_n}{\epsilon_i^2} \exp\left(-\frac{U_n}{2kT}\right) F(j_3 = 2), \quad (20)$$

$$F(j) = kT \left(\frac{U_n}{2}\right)^j + \sum_{i=1}^j j(j-1) \cdots (j-i+1) (kT)^{i+1} \left(\frac{U_n}{2}\right)^{j-i}, \quad (21)$$

and the threshold energy  $E_{\min} = U_n/2$  was taken for both the ionization and excitation collisions.

### 3. RATE COEFFICIENTS FROM OTHER THEORIES

#### 3.1. Semi-empirical Rate Coefficients

The Drawin semi-empirical rate coefficient for the direct ionization ( $n \rightarrow c$ ) and direct excitation ( $n \rightarrow n'$ ) of hydrogen atom upon impact of the ground state hydrogen atom are (see Drawin 1968, 1969 and Drawin & Emard 1973)

$$S_{nc}^H(T) = 64\pi a_0^2 \left(\frac{Ry}{U_n}\right)^2 \left(\frac{kT}{\pi m_H}\right)^{1/2} \frac{m_e}{m_H} \Psi(\omega_n), \quad (22)$$

$$C_{nn'}^H(T) = 64\pi a_0^2 \left(\frac{Ry}{\Delta E_{nn'}}\right)^2 f_{nn'} \left(\frac{kT}{\pi m_H}\right)^{1/2} \frac{m_e}{m_H} \Psi(\omega_{nn'}), \quad (23)$$

where

$$\omega_n = \frac{U_n}{kT}, \quad \omega_{nn'} = \frac{\Delta E_{nn'}}{kT}, \quad (24)$$

$$\Psi(x) = \left(1 + \frac{2}{x}\right) \left[ \frac{1}{1 + (2m_e/m_H x)^2} \right] \exp(-x). \quad (25)$$

The oscillator strengths  $f_{nn'}$  for the dipole allowed transitions in hydrogen can be approximated by (see, for example, Johnson 1972)

$$f_{nn'} = \frac{32}{3\pi\sqrt{3}} G_{nn'} n^{-5} n'^{-3} \left(\frac{1}{n^2} - \frac{1}{n'^2}\right)^{-3}, \quad (26)$$

where

$$G_{nn'} = \begin{cases} 0.75 & \text{for } n = 1 \\ 0.85 & \text{otherwise} \end{cases}. \quad (27)$$

The semi-empirical formulae appear in different forms in the literature. The formulae given by equations (22) and (23) seemed to be the most common interpretation of the semi-empirical results of Drawin (see also Fleischmann & Dehmel 1972 and Paper I for the interpretation of the semi-empirical cross sections).

#### 3.2. First-Order Exchange (Quantum-mechanical) Rate Coefficients

The following fits to the rate coefficients for the excitation transitions in collision of two ground-state hydrogen atoms using the first-order exchange approximation have been proposed by McLaughlin & Bell (1989)

$$C_{ln}^H(T) = \sum_l A(nl) T^{1/2}, \quad (28)$$

where the rate coefficient is in units of  $10^{-17} \text{ cm}^3 \text{ s}^{-1}$ ,  $T$  is in K and the constants  $A(nl)$  are given in Table 5 of McLaughlin & Bell (1989); the sum in equation (28) is taken over the orbital

quantum numbers  $l = s, p, d$ . All of the first-order exchange cross sections and rate coefficients of McLaughlin & Bell (1989, 1983) presented here, except for the  $1 \rightarrow 2$  transition, refer to

$$\text{H}(1s) + \text{H}(1s) \rightarrow \text{H}(\Sigma) + \text{H}(nl), \quad (29)$$

where  $\text{H}(\Sigma)$  indicates that the incident atom can be left, after the collision, in any bound or continuum state.

#### 3.3. Semiquantal Rate Coefficients

The semiquantal theory of Flannery (1970) for H-H excitation and ionization rate coefficients can also be compared with the results of the present work. Flannery (1970) also calculated the H-H excitation rate coefficients using Bates & Khare's theory (1965); therefore these rate coefficients are also compared here. The approach of Flannery (also assuming direct collisions) was developed for the excitation, deexcitation and ionization of highly excited ( $n \gg 1$ ) hydrogen atoms at thermal energies. In his approach, Flannery treated the H-H excitation and ionization collisions as a problem of  $e\text{-H}(1s)$  elastic scattering and the internal energy change of the electron (with respect to its ion) was evaluated using classical mechanics. Extension and refinement of the semiquantal theory to cover a wider class of transition and range of energy is discussed in Flannery (1972, 1973).

### 4. RESULTS AND DISCUSSION

The ionization and excitation cross sections of the present work are compared with available measurements and theories in Figures 1–9; the slight kinks at the lower energy region of

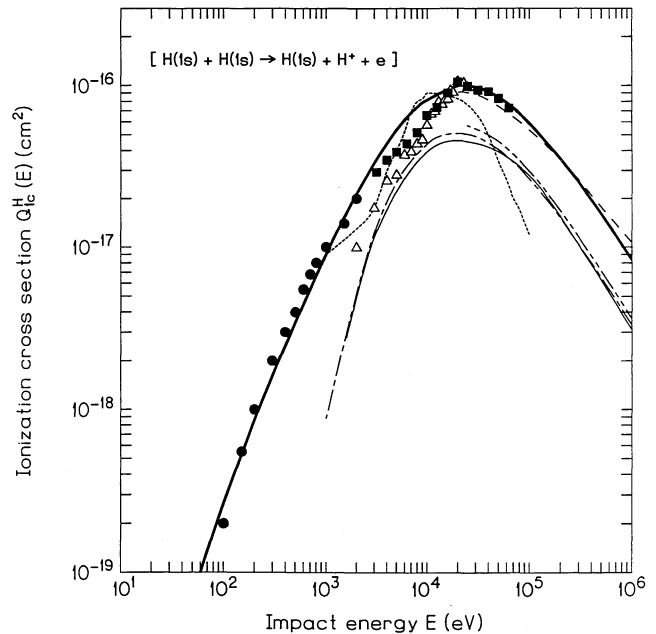


FIG. 1.—The direct ionization cross sections for collision of two ground-state hydrogen atoms. Thick solid curve represents the direct ionization cross section of the present work, while thin dashed curve is the classical impulse approximation cross section of Bates et al. (1969). Thin solid, dotted, dot-dashed, and double-dot-dashed curves represent the quantum-mechanical calculations of Bates & Griffing (1953), Shingal et al. (1989), Omidvar & Kyle (1970), and Flannery (1973), respectively. Experimental results are from Gealy & Van Zyl (1987; solid circles), Hill et al. (1979; open triangles), and McClure (1968; solid squares).

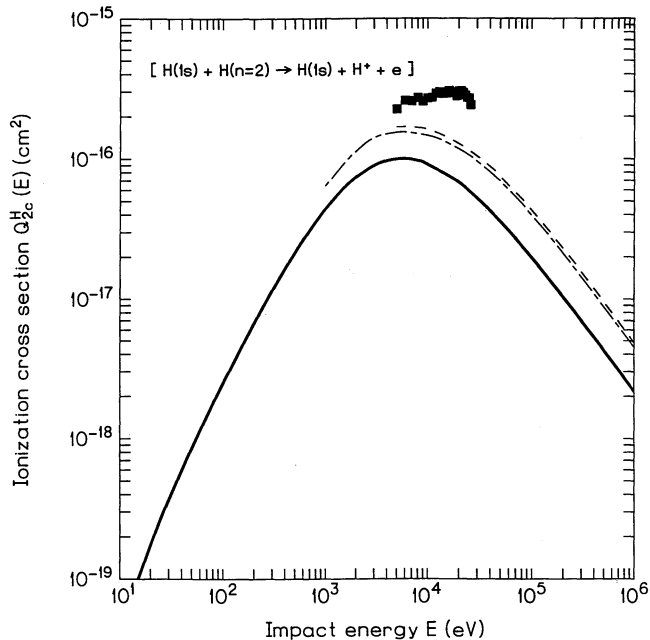


FIG. 2.—The cross sections for the direct ionization of hydrogen atom excited to the  $n = 2$  level upon impact of a ground-state hydrogen atom. Solid curve represents the cross section of the present work, and the solid squares represent the electron-loss cross sections of Hill et al. (1979) for  $H(2s) + H(1s) \rightarrow H^+ + e + H(\Sigma)$ , thin dashed and dot-dashed curves represent the quantum-mechanical calculations of Bell & Kingston (1971), and Omidvar & Kyle (1970), respectively.

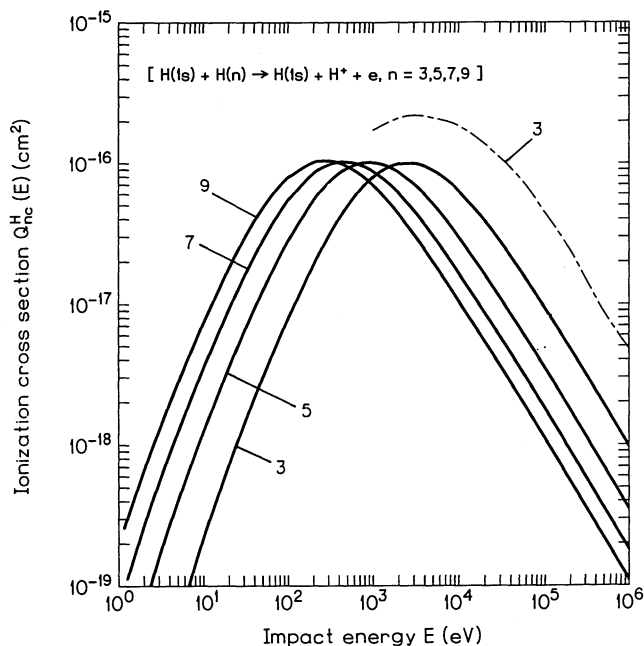


FIG. 3.—The cross sections (solid curves) for the direct ionization of hydrogen atom excited to the  $n = 3, 5, 7, 9$  levels upon impact of a ground-state hydrogen atom. Dot-dashed curve represents the quantum-mechanical calculation of Omidvar & Kyle (1970) for the direct ionization from the  $n = 3$  level.

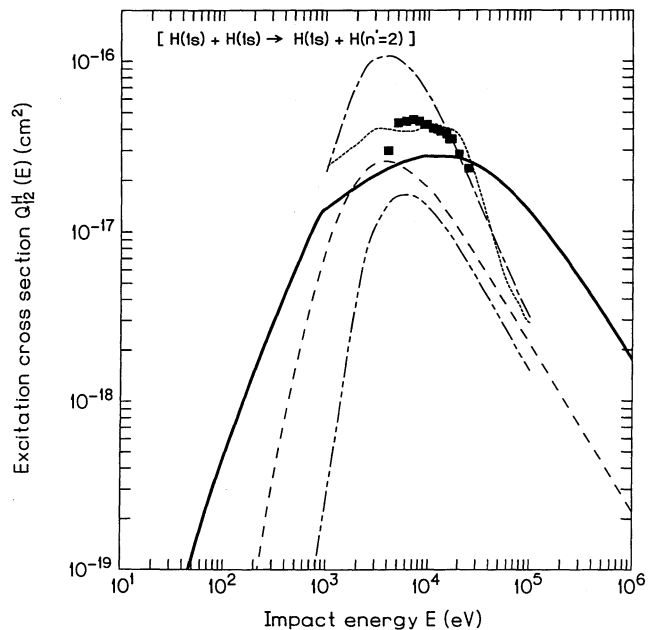


FIG. 4.—The cross sections for the direct excitation of the ground state ( $n = 1$ ) hydrogen atom to the  $n = 2$  level upon impact of a ground-state hydrogen atom. Solid curve represents the results of the present work, while dotted, dashed, dot-dashed, and double-dot-dashed curves represent the quantum-mechanical results of Shingal et al. (1989), Pomella (1967), McLaughlin & Bell (1983), and Flannery (1969b), respectively. The experimental results (solid squares) are from Morgan et al. (1974, 1980).

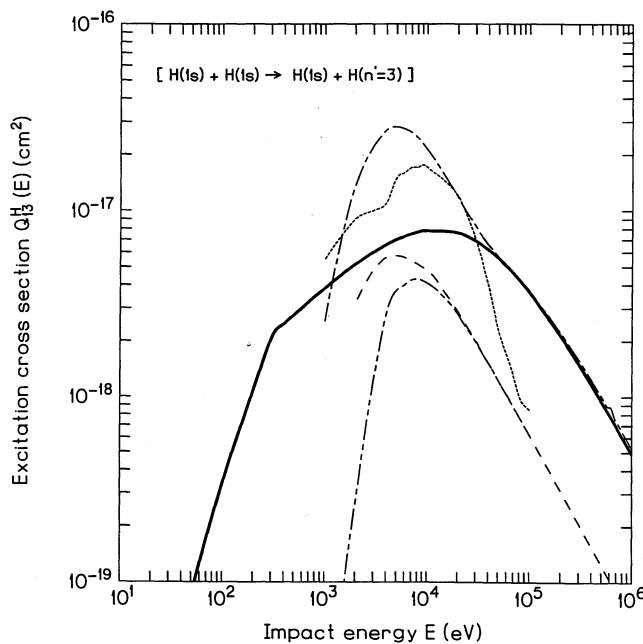


FIG. 5.—The cross sections for the direct excitation of the ground state ( $n = 1$ ) hydrogen atom to the  $n = 3$  level upon impact of a ground-state hydrogen atom. Solid curve represents the results of the present work, while dotted, dashed, dot-dashed, and double-dot-dashed curves represent the quantum-mechanical results of Shingal et al. (1989), Pomella (1967), McLaughlin & Bell (1989) [for  $H(1s) + H(1s) \rightarrow H(\Sigma) + H(n = 3)$ ], and Flannery (1969a), respectively.



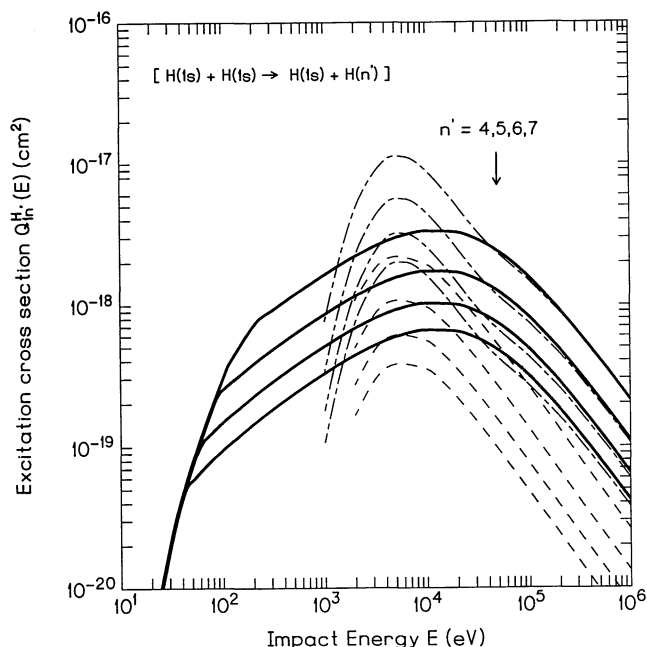


FIG. 6.—The cross sections for the direct excitation of the ground state ( $n = 1$ ) hydrogen atom to the  $n = 4, 5, 6, 7$  levels upon impact of a ground-state hydrogen atom. Solid curves represent the results for the present work, while dashed and dot-dashed curves represent the quantum-mechanical results of Pomella (1967), and McLaughlin & Bell (1989) [for  $H(1s) + H(1s) \rightarrow H(\Sigma) + H(n)$ ], respectively. The arrow indicates the direction of increasing  $n$  (4, 5, 6, and 7) for each set of cross sections.

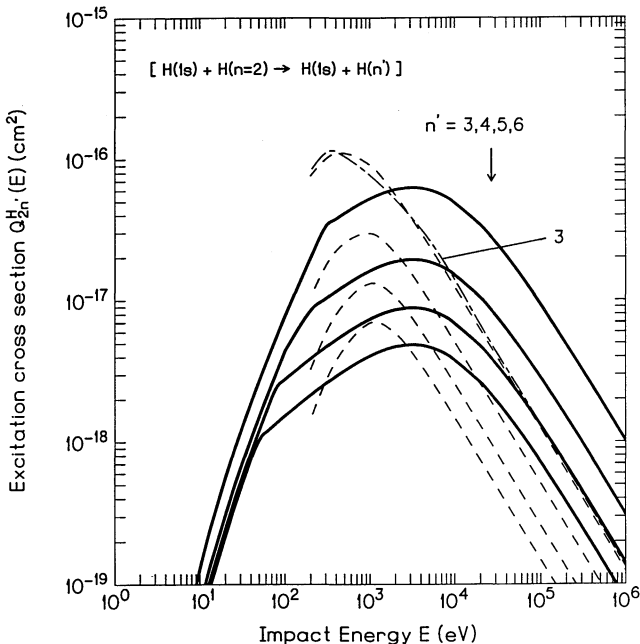


FIG. 8.—The cross sections for the direct excitation of the hydrogen atom from the  $n = 2$  level to the  $n = 3, 4, 5, 6$  levels upon impact of a ground-state hydrogen atom. Solid curves represent the results of the present work, while the dashed curves represent the quantum-mechanical results of Pomella (1967). Dot-dashed curve represents the semiquantal results of Flannery (1972) for  $2 \rightarrow 3$  transition. The arrow indicates the direction of increasing  $n$  (3, 4, 5, and 6) for each set of cross sections.

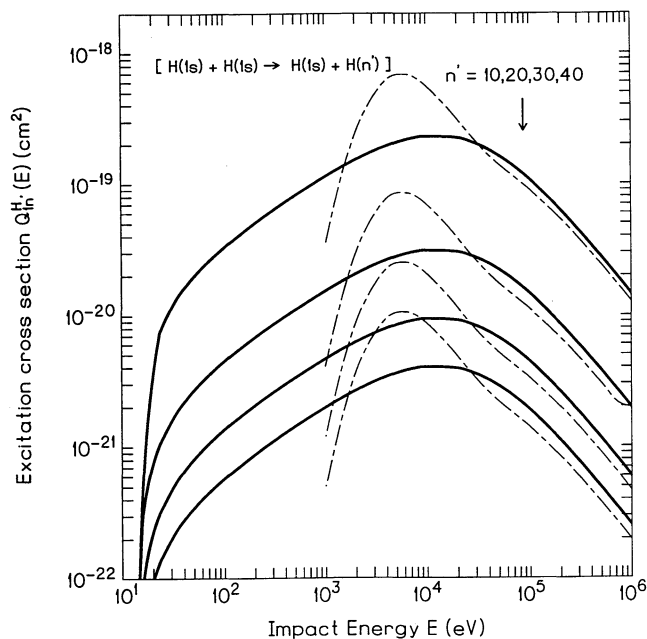


FIG. 7.—The cross sections for the direct excitation of the ground state ( $n = 1$ ) hydrogen atom to the  $n = 10, 20, 30, 40$  levels upon impact of a ground-state hydrogen atom. Solid curves represent the results of the present work and dot-dashed curves represent the quantum-mechanical results of McLaughlin and Bell (1989) for  $H(1s) + H(1s) \rightarrow H(\Sigma) + H(n)$ . The arrow indicates the direction of increasing  $n$  (10, 20, 30, and 40) for each set of cross sections.

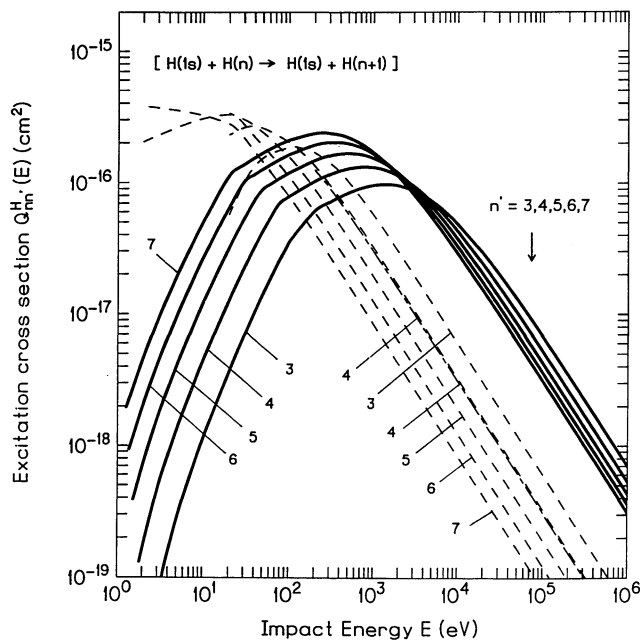


FIG. 9.—The cross sections for the direct excitation of the hydrogen atom from the  $n$ th level to the  $n' = n + 1$  level upon impact of the ground-state hydrogen atom. Solid curves represent the results of the present work, while dashed curves represent the quantum-mechanical results of Pomella (1967). Dot-dashed curve represents the semiquantal results of Flannery (1972) for  $4 \rightarrow 5$  transition. The arrow indicates the direction of increasing  $n$  (3, 4, 5, 6, and 7).

the excitation cross sections are due to the approximation (5). In general, the overall agreement (see Figs. 1, 2, and 4) of the maximum values of the classical impulse approximation ionization and excitation cross sections and the corresponding locations of the maxima with measurements (available, however, only for a limited number of H-H transitions) is good; all the results agree to within a factor of 2–3.

The present cross sections for the  $H(1s) + H(1s)$  direct ionization are in good agreement (see Fig. 1) with the low-energy ( $E \lesssim 2$  keV) experimental results of Gealy & Van Zyl (1987). The ionization cross sections also agree well with the data of Hill, Geddes & Gilbody (1979) and McClure (1968) at  $1 \text{ keV} \lesssim E \lesssim 70 \text{ keV}$ . The first-Born-approximation results of Omidvar & Kyle (1970) show that the contribution of double-transition collisions to the total cross section for the  $H(1s) + H(1s)$  ionizing collision is not significant in this energy range, varying from 10% at  $E = E_{1c}^* \approx 20 \text{ keV}$  to 50% at  $E = 75 \text{ keV}$ . The results of Omidvar & Kyle are in good agreement with the semiquantal results of Flannery (1973) and with the earlier Born approximation results of Bates & Griffing (1953, 1955). The present ionization cross sections are in better agreement with the close-coupling calculations of Shingal, Bransden, & Flower (1989) than with the results of Omidvar & Kyle (1970). Flannery (1973), and Bates & Griffing (1953) at  $1 \text{ keV} \lesssim E \lesssim 20 \text{ keV}$ . As discussed in Paper I, the present ionization cross sections overestimate the first Born approximation results by a factor of  $\sim 2$  at energies higher than 100 keV. It was pointed out in the earlier classical impulse approximation work of Bates, Dose, & Young (1969) and Paper I that this discrepancy is a result of the violation of the uncertainty principle when applying classical mechanics to the collision. (A comparison of the present collision model and that of Bates, Dose, & Young 1969 is given in Paper I).

The cross sections from the present work for the direct ionization from the excited levels of hydrogen atom are given in Figures 2 and 3. The trend of the first Born approximation cross sections of Omidvar & Kyle (1970) and Bell & Kingston (1971) agree with our cross sections for the direct ionization of the  $H(n=2)$  atoms (see Fig. 2). A similar statement can be made about the cross sections for the ionization from the  $n=3$  level (see Fig. 3). However, the high-energy cross sections for ionization from the  $n=2$  and 3 levels are still approximately a factor of 2–5 lower than the first-Born-approximation results of Omidvar & Kyle. (We should add that the first Born approximation results are in good agreement with the semiquantal results of Flannery 1972, not shown). The reliability of the classical impulse approximation cross section for these cases at high energies is similar to the case of ionization from the ground state.

The predicted energies of the maxima of the present cross sections for direct ionization are in good agreement with the first-Born-approximation results of Omidvar & Kyle (1970) for  $n=1, 2, 3$  (see Figs. 1, 2, and 3); however, the values of the maxima of the cross sections differ significantly. For the  $H(1s) + H(1s)$  ionization, the magnitude of the present cross section is in better agreement with the experimental values than with the first Born approximation results. The maxima of the present ionization cross sections are independent of  $n$  while the maxima of the first-Born-approximation cross sections are increasing functions of  $n$ . (Note that the present ionization cross sections at the lower energy range are proportional to  $n^3$ ; see eq. [10]). The feasibility of the constant ( $n$ -independent) maximum H-H direct ionization cross sections (particularly

relevant to ionization from highly excited levels) may be rationalized as follow. We first note that the maxima of the cross sections occur when the velocity of the incident H atom is almost equal to the field electron orbital speed. Scaling of the relative velocity between the H-H and  $e$ -H systems indicate that the locations of the maxima of the H-H ionization cross sections would correspond to the location of “maxima” of the  $e$ -H( $1s$ ) “elastic” cross section (around the threshold of the elastic cross section). In the limit of ionization from highly excited levels ( $n \gg 1$ ), the constant value of the maximum ionization cross sections seem to be consistent with the idea that the problem of  $H(n \gg 1)$ -H direct collision may be treated as the problem of electron-H( $1s$ ) elastic collision (see, for example, Flannery 1970). This is because the weakly bound electron in the highly excited hydrogen atoms can be treated as if it is free from the influence of the target nucleus. If the role of the target nucleus can be neglected during the  $H(n \gg 1)$ -H interaction then the maximum values of the H-H ionization cross section should correspond to the  $e$ -H total elastic cross section near the threshold. However, from the results of the present work, we note that the direct application of the model of free electron-H collision to the  $H(n \gg 1)$ -H collision may not be valid. This is because the  $e$ -H( $1s$ ) total elastic cross section near the threshold have value of  $\sim 3.6 \times 10^{-15} \text{ cm}^2$  and the maximum value of the present ionization cross section is about factor of 36 lower. This difference may be understood in terms of the target nucleus-incident  $H(1s)$  interaction (more or less taken into account in our collision model with the spatially averaged interaction potential used; see Paper I) whose effect is to reduce the effective cross section of the field electron –  $H(1s)$  elastic collision (see discussions in Flannery 1980, 1982 and Hahn 1982, 1981; both had argued and shown that in the thermal collisions of Rydberg atoms with neutrals, the perturbation due to the Rydberg core-neutral interaction can be significant). Also, we may add that some indirect evidence in support for the argument given above can be obtained from the roughly constant measured maximum H-H ionization cross sections (although limited to two available cases) for the ground-state and first excited state (Figs. 1 and 2).

Comparison of the excitation cross sections of the present work with the available experimental and theoretical work is given in Figures 4–9. The semiquantal, first Born approximation and the first-order exchange cross sections for the  $1 \rightarrow n$  excitation transitions (Figs. 4–7) decrease to zero at low energies at a much faster rate than the cross sections for the present work; the opposite trend can be seen (Fig. 9) in case of  $n \rightarrow n+1$  transitions at low energies. At medium energies, our cross sections are in better qualitative agreement with the experimental data of Morgan, Geddes, & Gilbody (1974) and Morgan, Stone, & Mayo (1980) (for  $1 \rightarrow 2$ ; see Fig. 4) and with the close-coupling calculations of Shingal, Bransden, & Flower (1989) (for  $1 \rightarrow 2, 1 \rightarrow 3$ ; see Figs. 4 and 5) than with the first Born approximation results of Pomella (1967), the semiquantal results of Flannery (1969a, b), and the first-order exchange calculations of McLaughlin & Bell (1989). At high energies, the classical impulse approximation and the first Born approximation excitation cross sections are both proportional to  $1/E$ . However, our results are larger than the first Born approximation cross sections of Pomella (1967) by a factor of  $\sim 10$  [for all the  $n \rightarrow n'$  ( $n < n' \leq 8$ ) transitions available for comparison].

A comparison of the classical impulse approximation excitation cross section for the  $n \rightarrow n+1$  ( $n=3, 4, 5, 6, 7$ ) transitions

with the first-Born results of Pomella (1967) is given in Figure 9. We should note that the semiquantal cross sections of Flannery (1972) agree well with the first Born cross sections for  $n = 2$  and 4 (see Figs. 8 and 9). One can see from Figure 9 that the general behavior of the  $n \rightarrow n + 1$  excitation cross section can be divided into two parts. At  $E < 5$  keV, the cross section increases with  $n$  while the opposite is true at  $E > 5$  keV (the  $n$ -dependence of the excitation cross sections at low-energy, at the maxima and at high-energy are given by equations (11), (7), and (13) to behave approximately as  $n^5$ ,  $n$ , and  $1/n$ , respectively). Such a behavior is different from electron-impact excitation where the excitation cross section is expected to increase with  $n$  at all energies (see, for example, Omidvar 1965). From Figure 9, we also note that the maxima of the first-Born excitation cross sections are shifted toward lower energies at a much faster rate than the present results.

All of the above comparisons for the ionization and excitation H-H cross sections have been so far restricted to processes (1) and (2); ionization and excitation of the target H atom upon impact of an incident H(1s) ground-state atom. In Figure 10, we also compare the present cross sections with the work of Flannery & McCann (1979) for  $H(n) + H(5) \rightarrow H(n) + H^+ + e$  where the incident H atom is in the excited  $n = 2, 3, 4$  levels. The overall agreement of the comparison is reasonable, but our ionization cross sections are lower than the semiquantal cross sections of Flannery & McCann (1979) by a factor of  $\sim 10$ . The comparison illustrates the ability of the present formulae to provide a quick estimate of the cross sections for some of the direct transitions in atom-atom collisions. Such estimates might be useful before performing complex computations (or even before the formulation of the collision model) in a more serious effort to understand the complex inelastic interactions between atoms.

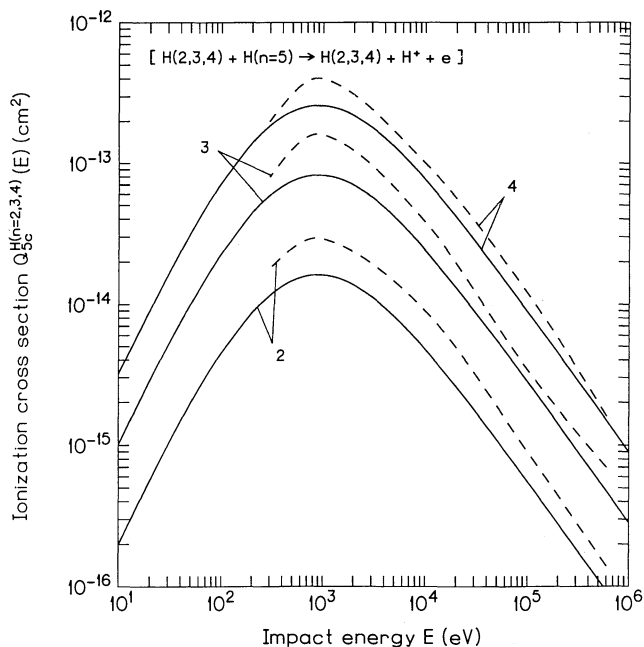


FIG. 10.—The cross sections of the direct ionization of hydrogen atom excited to the  $n = 5$  level upon impact of an excited hydrogen atom [ $H(n = 2, 3, 4) + H(n = 5) \rightarrow H(n = 2, 3, 4) + H^+ + e$ ]. Solid curves represent the results of the present work raised by a factor of 10 while dashed curves represent the semiquantal results of Flannery & McCann (1979).

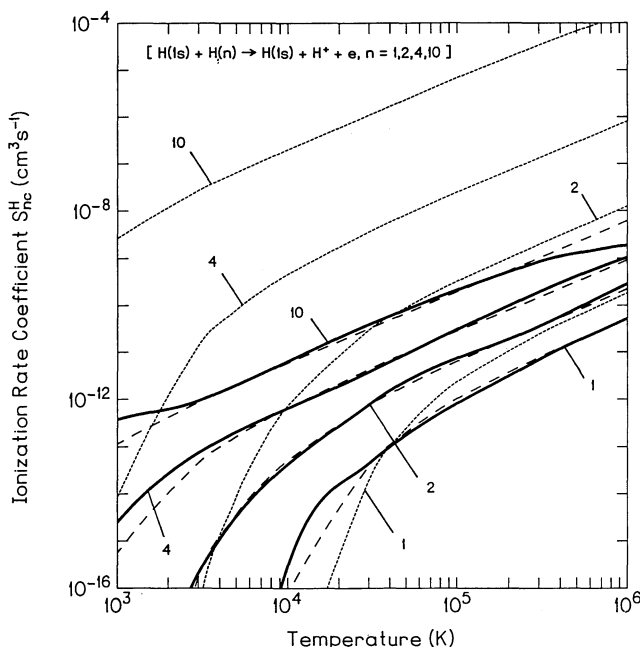


FIG. 11.—The rate coefficients for the direct ionization of hydrogen atom excited to the  $n = 1, 2, 3, 4, 10$  levels upon impact of the ground-state hydrogen atom. Solid curves are the rate coefficients of the present work obtained from direct numerical integration, while thin dashed curves are the approximate rate coefficients given by eq. (15). Thin dotted curves are the semi-empirical rate coefficients of Drawin (1969).

A comparison of the numerically integrated rate coefficients with the approximate formulae (15) and (16) is given in Figures 11–13. The ionization rate coefficients obtained from equation (15) agree to within a factor of a few (for all the  $n \leq 10$  transitions examined) with the numerically integrated results. The excitation rate coefficients obtained from equation (16) also agree to within a factor of a few with the numerically integrated results for all the excitation transitions (for the  $n < n' \leq 10$  transitions examined) except for the  $1 \rightarrow n'$  transitions. The comparison of the approximate excitation rate coefficients for the  $1 \rightarrow n'$  ( $n' \leq 10$ ) transitions with the numerical results can differ by as much as factor of 10 at  $T \gtrsim 10^5$  K (see discussion below). At this temperature range, the approximate formula (16) is not recommended, and the rate coefficients should be calculated by numerical integration of equation (14).

The applicability of the approximate analytical rate coefficients is limited to temperature ranges from  $10^3 \text{ K} \lesssim T \lesssim 10^6 \text{ K}$ . This is because at high temperatures ( $T \gtrsim 10^7 \text{ K}$ ) the rate coefficients depend on the medium- and high-energy parts of the cross sections whereas the approximate formulae consider only the contribution from the low-energy part of the cross section. Then direct numerical integration of the rate coefficients using the analytical cross sections is recommended. In addition, we also note that the high-energy part of the classical impulse approximation cross section of the present work is less reliable than the low and medium energy parts. Therefore, the rate coefficients calculated using the classical impulse approximation cross sections of the present work are not useful at temperatures  $T \gtrsim 10^7 \text{ K}$ .

Comparisons of the present rate coefficients with Drawin's semi-empirical formula for ionization and excitation are given in Figures 11–13. For the  $1 \rightarrow n$  excitation transitions, we also compare our rate coefficients with the results of McLaughlin &

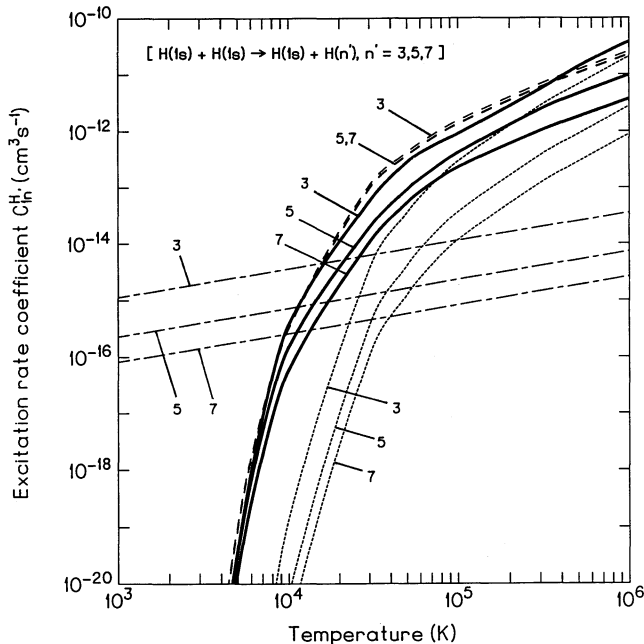


FIG. 12.—The rate coefficients for the direct excitation of the ground-state hydrogen atom to the  $n = 3, 5, 7$  levels upon impact of the ground-state hydrogen atom. Solid curves are the rate coefficients of the present work obtained from direct numerical integration, while thin dashed curves are the rate coefficients given by eq. (16). Thin dotted curves are the rate coefficients of Drawin (1969) and dot-dashed curves are the rate coefficients of McLaughlin & Bell (1989) [for  $H(1s) + H(1s) \rightarrow H(\Sigma) + H(n)$ ].

Bell calculated from formula (28) (see Fig. 12). The semi-empirical rates are considerably lower than our results and the McLaughlin & Bell results at lower temperatures. However, for direct ionization and excitation transitions involving the excited hydrogen atoms, the semi-empirical rate coefficients are much larger than our results (see Figs. 11 and 13). The comparison of our rate coefficients at low temperatures ( $T \lesssim 10^4$  K) with McLaughlin & Bell results also shows that the low temperature rate coefficients of the first order exchange results are most probably too high.

Comparisons of the numerically integrated rate coefficients for the ionization and excitation transitions involving highly excited states with the results of Flannery (1970), Bates & Khare (1965) and with the semi-empirical rate coefficients of Drawin (1968, 1969) are given in Tables 1 and 2. The comparison shows that the semi-empirical formula of Drawin significantly

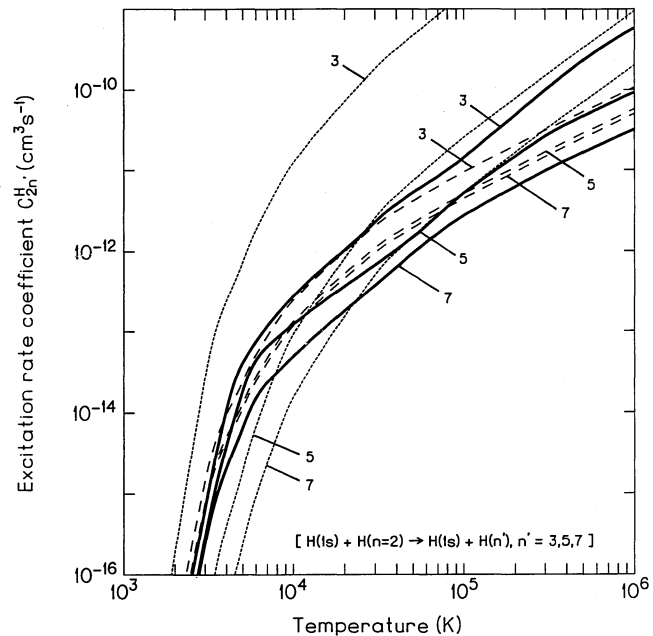


FIG. 13.—The rate coefficients for the direct excitation of a hydrogen atom from the  $n = 2$  level to the  $n = 3, 5, 7$  levels upon impact of the ground-state hydrogen atom. Solid curves are the rate coefficients of the present work obtained from direct numerical integration, while thin dashed curves are the rate coefficients given by eq. (16). Thin dotted curves are the semi-empirical rate coefficients of Drawin (1969).

cantly overestimates the rate coefficients for the transitions involving highly excited levels. Consequently, application of the semi-empirical formula to calculate the rate coefficients from these transitions is not recommended. The comparison of the trend of our ionization rate coefficients with the results of Flannery show good agreement between the two approaches; the rates are increasing functions of  $n$  at a given  $T$ . One conceivable explanation of the significant difference in the magnitude of the predicted rate coefficients would be the direct application of the  $e-H(1s)$  elastic threshold cross section in Flannery (1970) model for the  $H(n \gg 1)-H$  collision; it was noted in the previous discussion that this may overestimate the ionization cross sections. Keeping this possible difference in the magnitude of the rate coefficients in mind, we note the difference in the trend of our excitation rate coefficients with Flannery's results. For a given  $T$ , the semiquantal excitation

TABLE 1  
COMPARISON OF THE DIRECT IONIZATION RATE COEFFICIENTS  $S_{nc}^H$  ( $\text{cm}^3 \text{s}^{-1}$ ) FOR  $H(1s) + H(n) \rightarrow H(1s) + H^+ + e$

$n$	$T = 100 \text{ K}$			$T = 300 \text{ K}$			$T = 500 \text{ K}$		
	PW <sup>a</sup>	Flannery	Drawin	PW	Flannery	Drawin	PW	Flannery	Drawin
20	$8.18^{-16b}$	...	$7.30^{-10}$	$2.29^{-14}$	$1.01^{-14}$	$2.94^{-8}$	$7.86^{-14}$	$8.41^{-13}$	$9.01^{-8}$
30	$7.18^{-15}$	...	$4.71^{-8}$	$1.03^{-13}$	$2.54^{-12}$	$5.42^{-7}$	$3.08^{-13}$	$1.46^{-11}$	$1.34^{-6}$
40	$2.33^{-14}$	$8.98^{-14}$	$4.53^{-7}$	$2.64^{-13}$	$1.22^{-11}$	$3.55^{-6}$	$7.44^{-13}$	$4.04^{-11}$	$8.21^{-6}$
50	$5.22^{-14}$	$1.08^{-12}$	$2.17^{-6}$	$5.23^{-13}$	$2.67^{-11}$	$1.45^{-5}$	$1.42^{-12}$	$8.08^{-11}$	$3.25^{-5}$
60	$9.64^{-14}$	$3.64^{-12}$	$7.29^{-6}$	$8.92^{-13}$	$4.92^{-11}$	$4.47^{-5}$	$2.34^{-12}$	$1.27^{-10}$	$9.92^{-5}$
70	$1.58^{-13}$	$7.32^{-12}$	$1.97^{-5}$	$1.38^{-12}$	$7.31^{-11}$	$1.15^{-4}$	$3.50^{-12}$	$1.85^{-10}$	$2.53^{-4}$
80	$2.38^{-13}$	$1.25^{-11}$	$4.58^{-5}$	$1.97^{-12}$	$1.03^{-10}$	$2.60^{-4}$	$4.88^{-12}$	$2.44^{-10}$	$5.68^{-4}$
90	$3.40^{-13}$	$1.81^{-11}$	$9.54^{-5}$	$2.68^{-12}$	$1.42^{-10}$	$5.31^{-4}$	$6.45^{-12}$	$3.13^{-10}$	$1.16^{-3}$
100	$4.62^{-13}$	$2.53^{-11}$	$1.83^{-4}$	$3.49^{-12}$	$1.76^{-10}$	$1.01^{-3}$	$8.16^{-12}$	$3.70^{-10}$	$2.18^{-3}$
150	$1.41^{-12}$	$7.24^{-11}$	$2.18^{-3}$	$8.64^{-12}$	$3.79^{-10}$	$1.16^{-2}$	$1.77^{-11}$	$7.16^{-10}$	$2.50^{-2}$

<sup>a</sup> PW denotes present work. The rate coefficients obtained from numerical integration of the corresponding cross sections over the Maxwellian distribution.

<sup>b</sup> Exponent denotes the power of 10 by which the entry must be multiplied.



TABLE 2  
COMPARISON OF THE DIRECT EXCITATION RATE COEFFICIENTS  $C_{nn+1}^H$  ( $\text{cm}^3 \text{s}^{-1}$ ) FOR  $\text{H}(1s) + \text{H}(n) \rightarrow \text{H}(1s) + \text{H}(n+1)$

$n$	$T = 20 \text{ K}$				$T = 200 \text{ K}$				$T = 1000 \text{ K}$			
	PW <sup>a</sup>	Flannery	BK <sup>b</sup>	Drawin	PW	Flannery	BK	Drawin	PW	Flannery	BK	Drawin
10	...	...	...	...	$2.79^{-15}$	...	...	$1.22^{-7}$	$1.02^{-12}$	$2.54^{-9}$	$2.44^{-9}$	$2.71^{-6}$
15	...	...	...	...	$1.12^{-13}$	$1.19^{-9}$	$1.41^{-9}$	$9.83^{-6}$	$8.17^{-12}$	$5.92^{-9}$	$5.58^{-9}$	$1.33^{-4}$
20	...	...	...	...	$8.49^{-13}$	$3.16^{-9}$	$3.06^{-9}$	$1.82^{-4}$	$3.13^{-11}$	$5.88^{-9}$	$5.76^{-9}$	$2.20^{-3}$
30	$3.00^{-15}$	$3.90^{-10}$	$9.77^{-10}$	$2.44^{-4}$	$8.41^{-12}$	$3.87^{-9}$	$3.76^{-9}$	$1.02^{-2}$	$1.39^{-10}$	$3.41^{-9}$	$3.73^{-9}$	$1.16^{-1}$
40	$6.95^{-14}$	$1.67^{-9}$	$1.85^{-9}$	$4.96^{-3}$	$3.19^{-11}$	$2.79^{-9}$	$3.03^{-9}$	$1.75^{-1}$	$2.87^{-10}$	$1.85^{-9}$	$1.61^{-9}$	$1.89^0$
50	$4.39^{-13}$	$2.03^{-9}$	$2.06^{-9}$	$4.78^{-2}$	$7.28^{-11}$	$1.84^{-9}$	$1.23^{-9}$	$1.59^0$	$4.59^{-10}$	$1.07^{-9}$	$6.48^{-10}$	$1.50^1$
60	$1.54^{-12}$	$1.87^{-9}$	$1.95^{-9}$	$2.98^{-1}$	$1.24^{-10}$	$1.23^{-9}$	$1.23^{-9}$	$9.52^0$	$6.53^{-10}$	$6.39^{-10}$	$2.83^{-10}$	$6.90^1$
70	$3.88^{-12}$	$1.57^{-9}$	$1.71^{-9}$	$1.39^0$	$1.82^{-10}$	$8.26^{-10}$	$5.79^{-10}$	$4.24^1$	$8.66^{-10}$	$4.36^{-10}$	$1.36^{-10}$	$2.05^2$
80	$7.95^{-12}$	$1.26^{-9}$	$1.39^{-9}$	$5.27^0$	$2.39^{-10}$	$6.04^{-10}$	$3.23^{-10}$	$1.50^2$	$1.10^{-9}$	$3.00^{-10}$	$7.11^{-11}$	$4.47^2$
90	$1.40^{-11}$	$9.84^{-10}$	$1.05^{-9}$	$1.70^1$	$3.03^{-10}$	$4.42^{-10}$	$1.88^{-10}$	$4.32^2$	$1.34^{-9}$	$2.04^{-10}$	$3.99^{-11}$	$8.10^2$
100	$2.20^{-11}$	$8.02^{-10}$	$7.57^{-10}$	$4.85^1$	$3.74^{-10}$	$3.18^{-10}$	$1.14^{-10}$	$1.04^3$	$1.60^{-9}$	$1.59^{-10}$	$2.37^{-11}$	$1.31^3$
150	$7.90^{-11}$	$2.96^{-10}$	$1.43^{-10}$	$2.63^3$	$8.05^{-10}$	$1.06^{-10}$	$1.57^{-11}$	$1.35^4$	$2.90^{-9}$	$4.88^{-11}$	$3.16^{-12}$	$7.06^3$

<sup>a</sup> PW denotes present work. The rate coefficients obtained from numerical integration of the corresponding cross sections over the Maxwellian distribution.

<sup>b</sup> BK denotes the results calculated from Bates & Khare's theory (1965).

rate coefficient first increases with  $n$ , reaches a maximum and then decreases as  $n$  increases whereas the present results are strictly increasing function of  $n$ . Such distinctive differences in the trend show clearly the sensitivity of the rates to the behavior of the low- and medium-energy parts of the corresponding cross sections. As already pointed out, the  $n$ -dependence of the ionization and excitation cross sections can be quite different depending on the range of the collision impact energy. At these low temperature cases, the rate coefficients should depend only on the low- and medium-energy parts of the cross sections. The present cross sections for the  $n \rightarrow n' = n + 1$  excitation transitions are increasing functions of  $n$  at these energy ranges (see Fig. 9); therefore our rates are increasing functions of  $n$ .

The comparison of our ionization and excitation cross sections with other available results leads us to conclude that the single-transition collision model adopted in the present work is inadequate for  $E \gtrsim 100 \text{ keV}$  for H-H collisions. The first Born approximation should give a reliable description of the atom-atom collisions at high energies  $E \gtrsim 100 \text{ keV}$  (Bell & Kingston 1974), and the application of the direct ionization and excitation cross sections of the present work is limited to the low- and medium-energy range ( $E \lesssim 5E_{nc}^*$ , or  $5E_{nn}^*$ ). This is mainly due to the inherent weakness of the classical model used in the present work for the description of high-energy collisions. It is difficult to draw conclusions on the reliability of the present cross sections for the direct ionization and excitation collisions at low energies ( $E \lesssim 1 \text{ keV}$ ) since there is available only one set of comparison data. However, from a comparison of the

present cross section with the measurements of Gealy & Van Zyl (1987) for the direct ionization from ground state, it is clear that the present cross sections are more reliable at low energies than the first Born approximation. Indeed, comparison of our results with existing measurements and theoretical predictions at medium impact energies seems to indicate that the present cross sections are also reliable in this energy range. Therefore, the classical impulse approximation rate coefficients evaluated at  $100 \text{ K} \lesssim T \lesssim 10^6 \text{ K}$  should also be reliable. From a comparison of the rate coefficients, we recommend the classical impulse approximation rate coefficients over the semi-empirical rate coefficients of Drawin. This is because (1) the semi-empirical rate coefficients are too large for excitation and ionization transitions involving the excited states; particularly for those involving the highly excited levels (see, for example, Tables 1 and 2), (2) the overall reliability of the classical impulse approximation rate coefficients appears to be good over a very wide range of physical conditions (for transitions involving the ground-state atoms to highly excited atoms;  $100 \text{ K} \lesssim T \lesssim 10^6 \text{ K}$ ).

I would like to thank Alex Dalgarno and Joseph Kunc for valuable comments and their constant encouragements throughout the work. The support of Sallie Baliunas is greatly appreciated. This work was supported by a grant from the Scholarly Studies Program and Langley-Abbot fund of the Smithsonian Institution.

#### REFERENCES

- Bates, D. R., Dose, V., & Young, N. A. 1969, *J. Phys. B*, 2, 930  
 Bates, D. R., & Griffing, G. 1953, *Proc. Phys. Soc.*, 66, 961  
 ———. 1954, *Proc. Phys. Soc.*, 67, 663  
 ———. 1955, *Proc. Phys. Soc.*, 68, 90  
 Bates, D. R., & Khare, S. P. 1965, *Proc. Phys. Soc.*, 85, 231  
 Bell, K. L., & Kingston, A. E. 1971, *J. Phys. B*, 4, 162  
 ———. 1974, *Adv. Atomic Molec. Phys.*, 10, 53  
 Drawin, H. W. 1968, *Z. Phys.*, 211, 404  
 ———. 1969, *Z. Phys.*, 225, 483  
 Drawin, H. W., & Emard, F. 1973, *Phys. Lett. A*, 43, 333  
 Flannery, M. R. 1969a, *Phys. Rev.*, 183, 231  
 ———. 1969b, *Phys. Rev.*, 183, 241  
 ———. 1970, *Ann. Phys.*, 61, 465  
 ———. 1972, *J. Phys. B*, 5, 334  
 ———. 1973, *Ann. Phys.*, 79, 480  
 ———. 1980, *Phys. Rev. A*, 22, 2408  
 ———. 1982, *J. Phys. B*, 15, 3249  
 Flannery, M. R., & McCann, K. J. 1979, *Phys. Rev. A*, 19, 2206  
 Fleischmann, H. H., & Dehmel, R. C. 1972, *Z. Phys.*, 252, 435  
 Gealy, M. W., & Van Zyl, B. 1987, *Phys. Rev. A*, 36, 3100  
 Hahn, Y. 1981, *Phys. B*, 14, 985  
 ———. 1982, *J. Phys. B*, 15, 613  
 Hill, J., Geddes, J., & Gilbody, H. B. 1979, *J. Phys. B*, 12, 3341  
 Johnson, L. C. 1972, *ApJ*, 174, 227  
 Kunc, J. A. 1987, *Phys. Fluids*, 30, 2255  
 Kunc, J. A., & Soon, W. H. 1991, *J. Chem. Phys.*, 95, 5738 (Paper I)  
 Levy, H. 1969, *Phys. Rev.*, 184, 97  
 McClure, G. W. 1968, *Phys. Rev.*, 166, 22  
 McLaughlin, B. M., & Bell, K. L. 1983, *J. Phys. B*, 16, 3797  
 ———. 1989, *Phys. B*, 22, 763  
 Morgan, T. J., Geddes, J., & Gilbody, H. B. 1974, *J. Phys. B*, 7, 142  
 Morgan, T. J., Stone, J., & Mayo, R. 1980, *Phys. Rev. A*, 22, 1460  
 Omidvar, K. 1965, *Phys. Rev.*, 140A, 38  
 Omidvar, K., & Kyle, H. L. 1970, *Phys. Rev. A*, 2, 408  
 Pomilla, F. R. 1967, *ApJ*, 148, 559  
 Pomilla, F. R., & Milford, S. N. 1966, *ApJ*, 144, 1174  
 Shingal, R., Bransden, B. H., & Flower, D. R. 1989, *J. Phys. B*, 22, 855  
 Smith, R. C., Krishner, R. P., Blair, W. P., & Winkler, P. F. 1991, *ApJ*, 375, 652